RESEARCH ARTICLE | OCTOBER 21 2024

# Effect of surface alignment on electric-field-induced phase transitions in blue phases

Sumanyu Chauhan ; Markus Wahle ; Dieter Cuypers ; Grigory Lazarev ; Herbert De Smet



*APL Mater.* 12, 101114 (2024)
https://doi.org/10.1063/5.0228656

# Effect of surface alignment on electric-field-induced phase transitions in blue phases

Cite as: APL Mater. 12, 101114 (2024); doi: 10.1063/5.0228656
Submitted: 14 July 2024 • Accepted: 23 September 2024 •
Published Online: 21 October 2024



Sumanyu Chauhan,[1,2,a] Markus Wahle,[1] Dieter Cuypers,[2] Grigory Lazarev,[1] and Herbert De Smet[2]

## AFFILIATIONS

[1] Optical and Quantum Communication Laboratory, Huawei Munich Research Center, 80992 Munich, Germany
[2] Centre for Microsystems Technology (CMST), IMEC and Ghent University, 9052 Ghent, Belgium

[a] Author to whom correspondence should be addressed: Sumanyu.Chauhan@Huawei.com

## ABSTRACT

This study investigates the critical electric field thresholds required for phase transitions in the blue phases of liquid crystals (BPs) confined within vertical field switching cells. BPs are attractive for electro-optical applications due to their polarization-independent response and fast switching times; however; challenges remain regarding their limited temperature stability and previously reported high operational voltages. We employ a combined approach of polarized optical microscopy and electrical impedance analysis to identify the electric field thresholds triggering BP transitions to focal conic domains in cells with and without planar polyimide alignment layers. We show that surface alignment layers stabilize the blue phases and allow for higher applied electric fields before transitioning into the focal conic state. This suggests the possibility of a wider operational voltage range in thinner cells with alignment layers. These findings significantly improve our understanding of BPs, addressing key challenges and paving the way for their integration into advanced photonic devices, based on the CMOS technology.





## INTRODUCTION

Blue phases (BPs) of liquid crystals represent a unique class of materials with promising applications in next-generation optical devices. Existing between cholesteric liquid crystal (N*) and isotropic phase, BPs exhibit a cubic (BP1 and BP2) or amorphous (BP3) structure, leading to distinct optical properties. Their benefits include polarization-independent electro-optical response, based on the Kerr effect[1,2] and sub-millisecond response times,[3] making them attractive for photonic devices, e.g., liquid crystal on silicon (LCOS) spatial light modulators (SLMs).[4,5] Despite these advantages, pure BPs face limitations such as a narrow temperature stability range (≈0.5–3 °C),[6] which can be enhanced by nanoparticle doping,[7] and previously reported high operational voltages in polymer-stabilized BPs (or PS-BPs)[8] that hinder integration with standard CMOS circuits designed for lower voltages.

In contrast to nematic liquid crystals, typically employed for electro-optic applications, BPs do not experience the Fréedericksz transition under the application of an electric field because of the arrangement of the molecules in the double twisted cylinders (DTCs).[9] Instead, their switching mechanisms involve a sequence of transitions starting with the electro-optic Kerr effect and progressing to photo-elastic effects. Following this, the transitions proceed from electrostriction or cubic lattice deformation to focal conic domains (FCD). This final transition before entering the isotropic phase involves the dismantling of the DTCs inherent in their structure. Electric fields significantly affect BPs.[10–13] The effects of electric field on BPs, including color shifts (electrostriction) and transitions between the BP states, are dependent on the field strength and frequency and exhibit hysteresis.[14] In addition to electrostriction, electric fields can reorient lattice facets to manipulate BP color, enabling precise color control.[15]

Initially, research focused on color changes, but the Kerr effect, an electric-field-induced phenomenon, has become the most promising area.[3] This effect is observed in various BPs.[16,17] However, the factors influencing the Kerr effect's strength remain unclear.[18] Separating the Kerr effect from electrostriction is challenging since both depend similarly on the square of the field strength.[19,20] Studies show a two-stage response with fast and slow components.[19,21] Polymer-stabilized systems exhibit similar behavior, with the Kerr effect dominating the faster response. Notably, polymer stabilization seems to suppress electrostriction more than the Kerr effect.[21,22]

The Kerr effect has also been demonstrated without polymer stabilization of BPs, but the driving voltages have been very high (≈141 $V_{rms}$).[23] Such voltages are far too high for any kind of practical application using modern electronics components, e.g., LCOS-based SLM. Moreover, these studies have not ascertained that, at such high voltages, the material under test is still a BP system or in an unwound state. Surface alignment layers have been shown to improve the performance of BP systems,[24–26] but their effect on the critical field strength has not been studied. Therefore, it is important to characterize critical voltages or electric field thresholds of surface-aligned BP systems below which the devices should be driven so that the structural integrity of the materials is maintained.

The most deployed technology for the high-resolution SLMs today is LCOS. The maximum available voltages that digital and analog LCOS backplanes can support are relatively low and are typically further decreasing with the trend going toward smaller pixel sizes and, hence, finer process nodes at silicon foundries,[27,28] making PS-BP an impractical choice for light modulation. In contrast, pure BP shows promise for these applications. Our research indicates that pure BPs, created using standard nematic hosts in thin cells, can function effectively at much lower voltages, compatible with the backplanes of commercial LCOS devices. However, it is also found that unwanted phase changes can be triggered at much lower voltages in that case. Therefore, it is crucial to monitor the structural integrity of pure BP under electrical fields. Specifically, we need to identify the critical voltage that causes BP to transition into focal conic domains (FCDs) before these materials can be reliably used and evaluated for light modulation in practical settings.

This study reports that surface alignment influences the electric field threshold for BP phase transitions. Instead of using techniques that require complex microscopic setups, such as Kossel patterns to validate BPs,[29] our method combines polarized optical microscopy (POM) for texture analysis[30] and permittivity measurements to distinguish BPs from N* and FCDs. This approach accurately identifies critical thresholds, preventing misinterpretations due to BP-to-FCD transitions at higher voltages.

## EXPERIMENTAL METHODS AND DESIGN

The BP mixture consisted of a nematic liquid crystal blend [HTG135400-100 from Jiangsu Hecheng Display Technology Co., Ltd. (HCCH) with electrical parameters: $e_{\parallel}$ = 49.6, $e_{\perp}$ = 11.5, and $\Delta e$ = 38.1] doped with 3.04 wt. % of the chiral dopant S5011 (from HCCH) with high helical twisting power (HTP = 126 $\mu m^{-1}$). This high HTP chiral dopant was used to stabilize the BP system for a long shelf life.[31] Samples were prepared in various vertical field switching (VFS) cell configurations for studying the phase transition temperatures of the binary nematic-chiral dopant mixtures. Commercial glass-ITO cells (from EHC, Japan) with thicknesses of 2 and 6 $\mu$m were used, with surface treatment (ST) and without surface treatment (NST). ST cells were processed with homogeneous alignment using a polyimide (PI) layer. Linkam LTS 120 heat stage and T-96 temperature controller were used to precisely regulate the temperature of the BP cells. BP textures formed during cooling were captured with a Leica DM2700M POM equipped with a camera. ITO electrodes provided a 10 × 10 $mm^2$ viewing area. The permittivity of BPs and N* was measured using a Rohde and Schwarz LCX100 LCR meter. The voltage range on the LCR meter was limited to a maximum value of 7 $V_{rms}$. All electrical measurements were conducted at a fixed sine wave frequency of 1 kHz.

## RESULTS AND DISCUSSIONS

The phase diagram in Fig. 1 illustrates the behavior of BP within glass-ITO transmissive cells of varying thicknesses, both with and without surface alignment. Cells with an alignment layer reach a higher isotropic temperature due to the alignment layer promoting a preferential orientation among the molecules. Consequently, more thermal energy is required to overcome this surface-alignment-induced orientational order and achieve the isotropic state compared to cells lacking such alignment. In this composition, BPs are typically stable within the temperature range of 71–74 °C (here we do not distinguish between BP1 and BP2).

Figure 2 presents POM images that show the features of BP[30] as it undergoes morphological changes under varying voltages. The

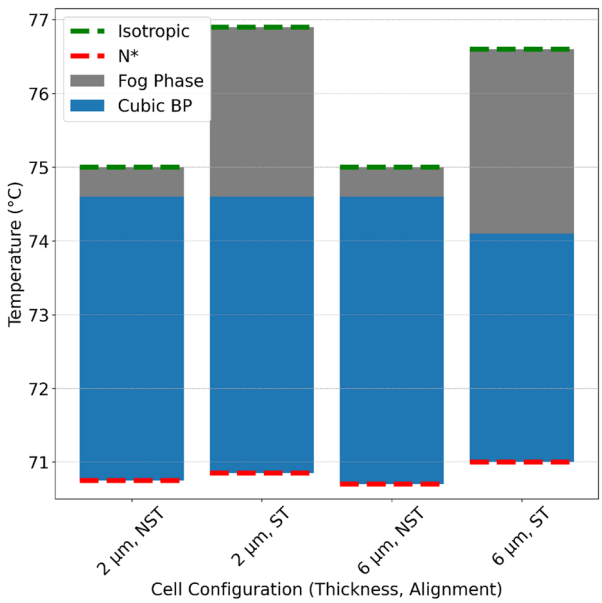


**FIG. 1.** Phase diagram illustrating the behavior of BPs in glass cells of varying thickness, with (ST) and without surface alignment (NST).

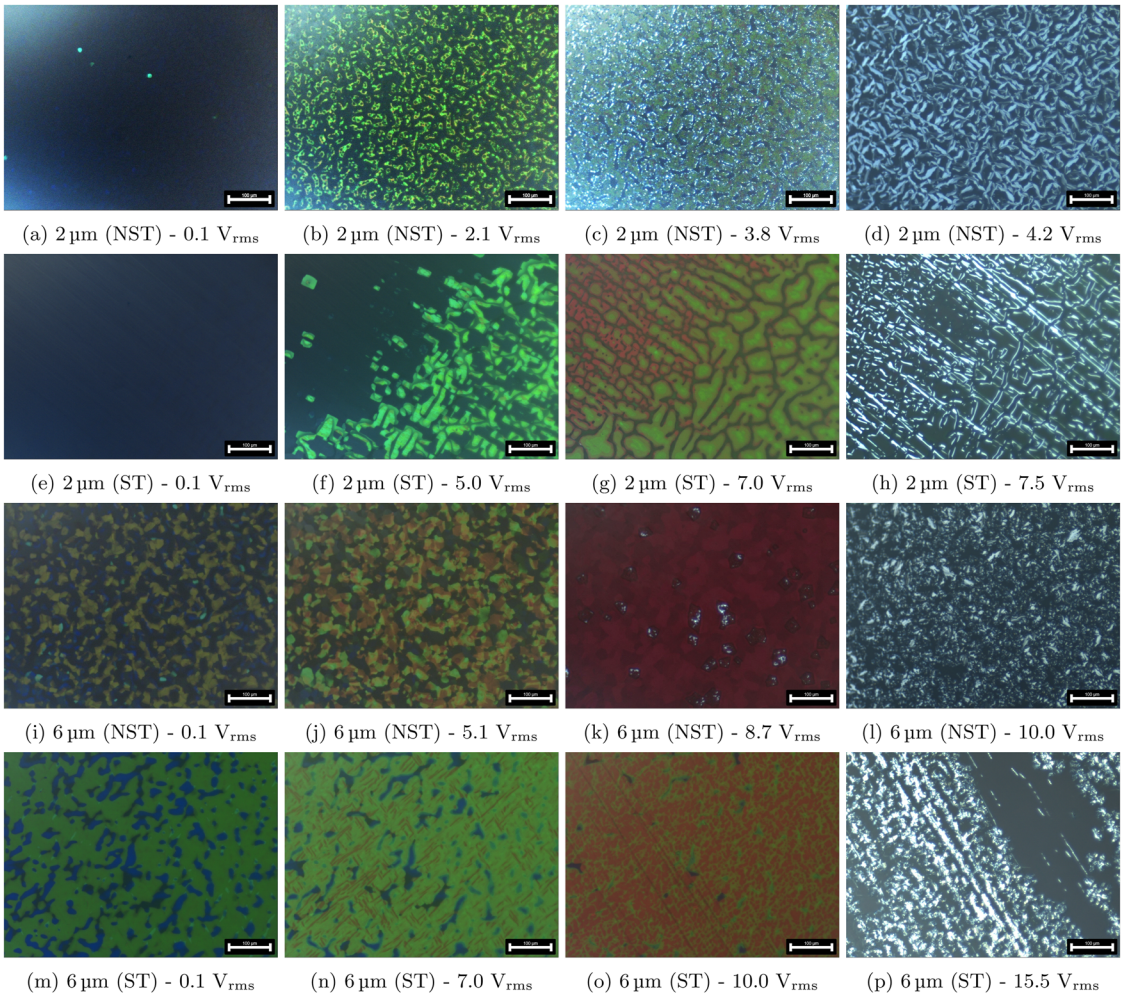


**FIG. 2.** POM images of electric-field-induced phase transition in BP inside 2 and 6 $\mu$m glass cells, either surface-treated (ST) for homogeneous alignment or non-surface-treated (NST). The test temperature was set at 73.0 °C. Scale bar: 100 $\mu$m. (a) 2 µm (NST) - 0.1 $V_{rms}$. (b) 2 µm (NST) - 2.1 $V_{rms}$. (c) 2 µm (NST) - 3.8 $V_{rms}$. (d) 2 µm (NST) - 4.2 $V_{rms}$. (e) 2 µm (ST) - 0.1 $V_{rms}$. (f) 2 µm (ST) - 5.0 $V_{rms}$. (g) 2 µm (ST) - 7.0 $V_{rms}$. (h) 2 µm (ST) - 7.5 $V_{rms}$. (i) 6 µm (NST) - 0.1 $V_{rms}$. (j) 6 µm (NST) - 5.1 $V_{rms}$. (k) 6 µm (NST) - 8.7 $V_{rms}$. (l) 6 µm (NST) - 10.0 $V_{rms}$. (m) 6 µm (ST) - 0.1 $V_{rms}$. (n) 6 µm (ST) - 7.0 $V_{rms}$. (o) 6 µm (ST) - 10.0 $V_{rms}$. (p) 6 µm (ST) - 15.5 $V_{rms}$.

images were captured for 2 and 6 µm cells, both with and without surface treatment. For the 2 µm non-surface-treated (NST) cell [see Figs. 2(a)–2(d)], at 73 °C and 0.1 $V_{rms}$, the sample displays a predominantly dark blue color, which is indicative of a mostly uniformly oriented pristine blue phase with some platelets reflecting green color [Fig. 2(a)]. As the voltage increases, the lattice structure reorients or experiences electrostriction, changing colors due to the Bragg reflection. The FCD starts at 3.8 $V_{rms}$ and manifests fully at 4.2 $V_{rms}$. For the 2 µm surface-treated (ST) cell with rubbed polyimide [see Figs. 2(e)–2(h)], a pristine blue phase without randomly oriented lattices is observed at 0.1 $V_{rms}$. The voltage threshold for inducing the FCD is higher, with the FCD appearing at 7.5 $V_{rms}$. This suggests that the alignment layer stabilizes the lattice structures, requiring higher voltages for phase transitions. In the 6 µm NST cell [Figs. 2(i)–2(l)], the BP shows diverse colors at 0.1 $V_{rms}$, which is indicative of a randomly oriented cubic BP lattice. As the voltage increases, the texture remains consistent while the colors shift, indicating electrostriction. The FCD transition occurs at 10.0 $V_{rms}$. For the 6 µm ST cell [Figs. 2(m)–2(p)], the BP exhibits less random orientation due to surface anchoring. Changes in the texture and color at higher voltages indicate electrostriction. The FCD transition starts at 14.5 $V_{rms}$ and manifests fully at a much higher voltage of 15.5 $V_{rms}$, highlighting the enhanced stability due to the alignment layer [Fig. 2(p)].

The subfigures in Fig. 3 present permittivity plots for BP measured at 73 °C (red) and N* measured at 27 °C (blue) for various cell configurations: a 2 µm NST cell [Fig. 3(a)], a 2 µm ST cell [Fig. 3(b)], a 6 µm NST cell [Fig. 3(c)], and a 6 µm ST cell [Fig. 3(d)]. LCR meter measurements were conducted over a macroscopic area of ~1 $cm^2$ on the ITO electrode, representing a broad assessment of the entire

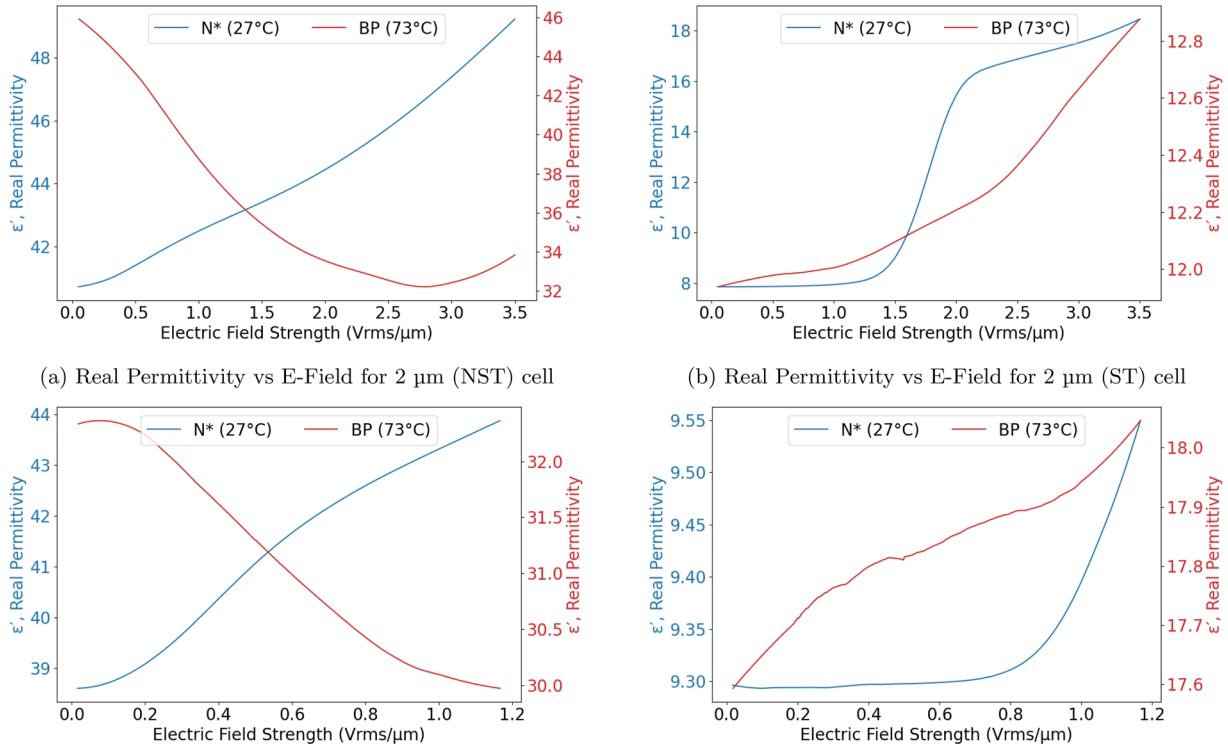


(a) Real Permittivity vs E-Field for 2 μm (NST) cell

(b) Real Permittivity vs E-Field for 2 μm (ST) cell

(c) Real Permittivity vs E-Field for 6 μm (NST) cell

(d) Real Permittivity vs E-Field for 6 μm (ST) cell

**FIG. 3.** Comparative electric-field-strength-dependent permittivity measurements for N* and BP in various cell configurations. N* measurements were made at 27 °C. BP measurements were made at 73 °C. (a) Real permittivity vs electric field for 2 μm (NST) cell. (b) Real permittivity vs electric field for 2 μm (ST) cell. (c) Real permittivity vs electric field for 6 μm (NST) cell. (d) Real permittivity vs electric field for 6 μm (ST) cell.

electrode surface. Hence, capacitance or permittivity measurements provide a coarse-grained view of the BP state.

In Figs. 3(a) and 3(c), the blue curves represent the permittivity of N* in FCD, indicative of a disordered system without switching thresholds due to the absence of alignment layers. In Figs. 3(b) and 3(d), the N* is in a planar state with higher order and visible switching electric field thresholds of 1.25 $V_{rms}/\mu m$ and 0.9 $V_{rms}/\mu m$, respectively. In all cases, the permittivity of N* increases with increasing electric field strength. For BP, in Figs. 3(a) and 3(c), there is no threshold switching in the disordered system, with a general decrease in the capacitance or real permittivity. The change in the slope of BP permittivity at an electric field value of ≈2.8 $V_{rms}$ $\mu m^{-1}$ in Fig. 3(a) indicates a transition to FCD and supports the observation of POM, the reported voltage, and field strength values in Figs. 2(d) and 4(b). In Fig. 3(b) and 3(d), although the alignment provides some preferential orientation and order, there is no Fréedericksz transition in BP regardless of surface anchoring, as the angle between the LC director and the electric field is arbitrary. Therefore, permittivity measurements can distinguish BP from N* due to the thresholdless response of BP in both aligned and unaligned cell configurations and the anomalous capacitance response[32]—for BP in the aligned state, there is a small increase in the capacitance, whereas for BP in the unaligned geometry, there is a general decrease in the capacitance.

Figure 4 summarizes the voltage ($V_{rms}$) and electric field ($V_{rms}$ $\mu m^{-1}$) thresholds required to induce the BP transition to FCD. As expected for dielectric materials, thicker cells require higher voltages to induce the transition due to the need for greater electrical energy to polarize the material and reorient the molecules [Fig. 4(a)]. Notably, the highest voltage threshold for the BP to FCD transition occurs at around 73 °C, corresponding to the middle of the BP temperature range where the lattice is most stable (see Fig. 1). The lowest voltage threshold is observed near the BP to N* transition at around 71 °C. Cells with an alignment layer require higher voltages for the transition due to the anchoring effect that stabilizes the lattice.

In practical LC devices where cell thickness is uniform, electric field strength ($V_{rms}$ $\mu m^{-1}$) is a crucial parameter for analyzing BP behavior. This measurement accounts for the uniform thickness of LC devices and the intrinsic properties of the device, such as permittivity, which are independent of thickness. As depicted in Fig. 4(b), cells lacking an alignment layer show similar electric-field-strength thresholds across different temperatures, demonstrating a consistent behavior pattern. In contrast, cells with alignment layers possess significantly higher electric-field-strength thresholds due to the

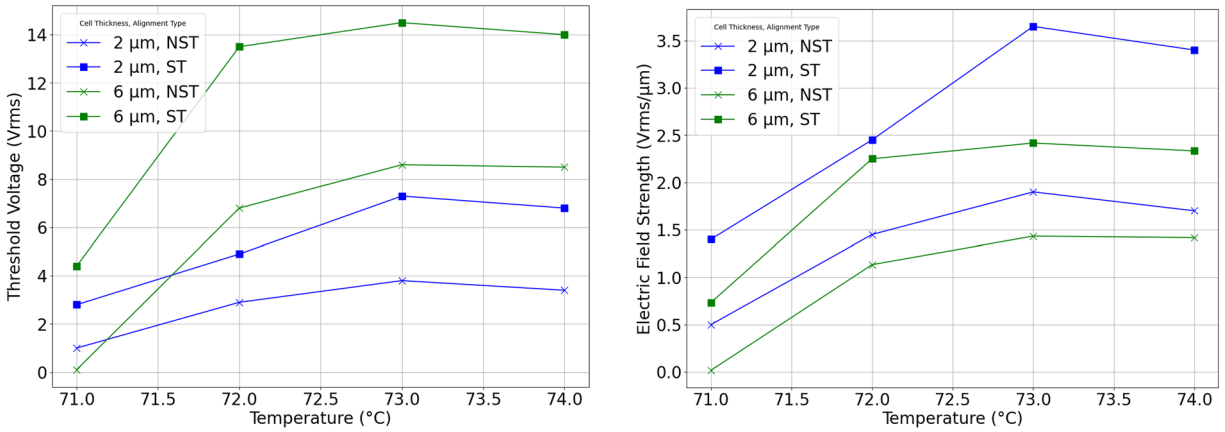


(a) Voltage-temperature response of BPs (b) E-field-temperature response of BPs

**FIG. 4.** Voltage-temperature and electric-field-strength-temperature responses of BP confined in varying cell configurations—either surface-treated (ST) for homogeneous alignment or non-surface-treated (NST), in 2 and 6 µm cells. (a) Voltage–temperature response of BPs. (b) Electric field–temperature response of BPs.

surface anchoring effect, which enhances the lattice order and stability. Furthermore, thinner, 2 µm cells consistently exhibit higher field-strength thresholds for BP to FCD transitions compared to their 6 µm counterparts. This could be due to stabilization effects from the closer spacing of the glass substrates or the strain tensor for the predominant and preferential lattice orientation[33] being able to withstand higher electric field strengths before transitioning to FCD.

## CONCLUSION

This study investigated the critical electric field thresholds that induce undesired phase transitions in pure BPs (from BPs to FCDs) confined within VFS cells of different cell thicknesses with and without planar alignment. By employing a combination of polarized optical microscopy and permittivity measurements, the BP state was distinguished from the $N^*$ phase. Thresholdless switching was demonstrated in both unaligned and aligned BP, indicating the inherent disorder and lack of symmetry breaking in the BP system.

The electrical field threshold in pure BP without alignment is barely exceeding ≈1.5–2 $V_{rms}\ \mu m^{-1}$. Surface alignment layers significantly increase the electric field threshold to ≈2.5–3.5 $V_{rms}\ \mu m^{-1}$ so that a wider operational voltage range becomes possible. The effect is especially strong in thin cells with alignment layers. These findings offer valuable insights for the design of future BP-based SLMs using high-resolution CMOS backplanes and approaches of micro-display technology.

## AUTHOR DECLARATIONS

### Conflict of Interest

The authors have no conflicts to disclose.

### Author Contributions

S.C. conceived and conducted the experiments. S.C., M.W., and D.C. analyzed the results. M.W., H.D.S., and G.L. reviewed the manuscript.

**Sumanyu Chauhan:** Conceptualization (equal); Data curation (equal); Formal analysis (equal); Investigation (equal); Methodology (equal); Validation (equal); Visualization (equal); Writing – original draft (equal); Writing – review & editing (equal). **Markus Wahle:** Methodology (supporting); Supervision (lead); Validation (equal); Writing – review & editing (lead). **Dieter Cuypers:** Supervision (supporting). **Grigory Lazarev:** Writing – review & editing (supporting). **Herbert De Smet:** Writing – review & editing (equal).

## DATA AVAILABILITY

The data that support the findings of this study are available from the corresponding author upon reasonable request.

## REFERENCES

[1] D. Chu, N. Collings, J. Moore, M. Pivnenko, and B. Robertson, European Patent No. EP 2807519 A1 (3 December 2014).
[2] S. Chauhan, M. Wahle, G. Lazarev, D. Cuypers, and H. D. Smet, "An experimental study of optical anisotropy of blue-phase liquid crystals as a function of alignment layers," Proc. SPIE **12417**, 1241717 (2023).
[3] Y. Chen and S.-T. Wu, "Recent advances on polymer-stabilized blue phase liquid crystal materials and devices," J. Appl. Polym. Sci. **131**, 4525 (2014).
[4] R. M. Hyman, A. Lorenz, S. M. Morris, and T. D. Wilkinson, "Polarization-independent phase modulation using a blue-phase liquid crystal over silicon device," Appl. Opt. **53**, 6925–6929 (2014).
[5] F. Peng, Y.-H. Lee, Z. Luo, and S.-T. Wu, "Low voltage blue phase liquid crystal for spatial light modulators," Opt. Lett. **40**, 5097–5100 (2015).
[6] H. J. Coles and M. N. Pivnenko, "Liquid crystal 'blue phases' with a wide temperature range," Nature **436**, 997–1000 (2005).
[7] K. Orzechowski, M. Tupikowska, O. Strzeżysz, T.-M. Feng, W.-Y. Chen, L.-Y. Wu, C.-T. Wang, E. Otón, M. M. Wójcik, M. Bagiński, P. Lesiak, W. Lewandowski, and T. R. Woliński, "Achiral nanoparticle-enhanced chiral twist and thermal stability of blue phase liquid crystals," ACS Nano **16**, 20577–20588 (2022).
[8] Y. Chen, D. Xu, S.-T. Wu, S.-i. Yamamoto, and Y. Haseba, "A low voltage and submillisecond-response polymer-stabilized blue phase liquid crystal," Appl. Phys. Lett. **102**, 141116 (2013).

[9]H. Ma, R. Yang, and Y. Sun, "The optical threshold and saturation voltage of blue-phase liquid crystal display with uniform operating electric field," Liq. Cryst. **42**, 1743–1747 (2015).
[10]H. Kitzerow, "The effect of electric fields on blue phases," Mol. Cryst. Liq. Cryst. **202**, 51–83 (1991).
[11]D. Armitage and R. Cox, "Liquid crystal blue phase to isotropic transition and electric field response," Mol. Cryst. Liq. Cryst. **64**, 41–50 (1980).
[12]P. Finn and P. Cladis, "Cholesteric blue phases in mixtures and in an electric field," Mol. Cryst. Liq. Cryst. **84**, 159–192 (1982).
[13]G. Heppke, M. Krumrey, and F. Oestreicher, "Observation of electro-optical effects in blue phase systems," Mol. Cryst. Liq. Cryst. **99**, 99–105 (1983).
[14]O. Henrich, D. Marenduzzo, K. Stratford, and M. Cates, "Thermodynamics of blue phases in electric fields," Phys. Rev. E **81**, 031706 (2010).
[15]H. Gleesson, R. Simon, and H. Coles, "Electric field effects and two frequency colour switching in the cholesteric and blue phases of nematic/cholesteric mixtures," Mol. Cryst. Liq. Cryst. **129**, 37–52 (1985).
[16]J. Yan, H.-C. Cheng, S. Gauza, Y. Li, M. Jiao, L. Rao, and S.-T. Wu, "Extended kerr effect of polymer-stabilized blue-phase liquid crystals," Appl. Phys. Lett. **96**, 071105 (2010).
[17]Y. Hisakado, H. Kikuchi, T. Nagamura, and T. Kajiyama, "Large electro-optic kerr effect in polymer-stabilized liquid-crystalline blue phases," Adv. Mater. **17**, 96–98 (2005).
[18]P. R. Gerber, "Electro-optical effects of a small-pitch blue-phase system," Mol. Cryst. Liq. Cryst. **116**, 197–206 (1985).
[19]H. Yoshida, S. Yabu, H. Tone, Y. Kawata, H. Kikuchi, and M. Ozaki, "Secondary electro-optic effect in liquid crystalline cholesteric blue phases," Opt. Mater. Express **4**, 960–968 (2014).
[20]Y. Zhang, H. Yoshida, Q.-H. Wang, and M. Ozaki, "Electro-optics of blue phase liquid crystal in field-perpendicular direction," Appl. Phys. Lett. **122**, 161107 (2023).
[21]D. Xu, J. Yan, J. Yuan, F. Peng, Y. Chen, and S.-T. Wu, "Electro-optic response of polymer-stabilized blue phase liquid crystals," Appl. Phys. Lett. **105**, 011119 (2014).
[22]H. Coles and H. Gleeson, "Electric field induced phase transitions and colour switching in the blue phases of chiral nematic liquid crystals," Mol. Cryst. Liq. Cryst. Incorporating Nonlinear Opt. **167**, 213–225 (1989).
[23]L. Tian, J. W. Goodby, V. Görtz, and H. F. Gleeson, "The magnitude and temperature dependence of the Kerr constant in liquid crystal blue phases and the dark conglomerate phase," Liq. Cryst. **40**, 1446–1454 (2013).
[24]S.-A. Jiang, W.-J. Sun, S.-H. Lin, J.-D. Lin, and C.-y. Huang, "Optical and electro-optic properties of polymer-stabilized blue phase liquid crystal cells with photoalignment layers," Opt. Express **25**, 28179–28191 (2017).
[25]P.-J. Chen, M. Chen, S.-Y. Ni, H.-S. Chen, and Y.-H. Lin, "Influence of alignment layers on crystal growth of polymer-stabilized blue phase liquid crystals," Opt. Mater. Express **6**, 1003–1010 (2016).
[26]K. Orzechowski, M. W. Sierakowski, M. Sala-Tefelska, P. Joshi, T. R. Woliński, and H. De Smet, "Polarization properties of cubic blue phases of a cholesteric liquid crystal," Opt. Mater. **69**, 259–264 (2017).
[27]G. Lazarev, P.-J. Chen, J. Strauss, N. Fontaine, and A. Forbes, "Beyond the display: Phase-only liquid crystal on silicon devices and their applications in photonics [Invited]," Opt. Express **27**, 16206–16249 (2019).
[28]G. Lazarev, A. Hermerschmidt, S. Krüger, and S. Osten, "LCOS spatial light modulators: Trends and applications," in *Optical Imaging and Metrology*, edited by W. Osten and N. Reingand (Wiley, 2012).
[29]B. Jérôme and P. Pieranski, "Kossel diagrams of blue phases," Liq. Cryst. **5**, 799–812 (1989).
[30]I. Dierking, *Textures of Liquid Crystals* (John Wiley & Sons, 2003).
[31]P. Joshi, J. De Smet, X. Shang, O. Willekens, D. Cuypers, G. Van Steenberge, O. Chojnowska, P. Kula, S. Van Vlierberghe, P. Dubruel *et al.*, "Long term stability of polymer stabilized blue phase liquid crystals," J. Disp. Technol. **11**, 703–708 (2015).
[32]P. Nayek, N. H. Park, S. C. Noh, S. H. Lee, H. S. Park, H. J. Lee, C.-T. Hou, T.-H. Lin, and H. Yokoyama, "Analysis of surface anchored lattice plane orientation in blue phase liquid crystal and its in-plane electric field-dependent capacitance response," Liq. Cryst. **42**, 1111–1119 (2015).
[33]H.-S. Kitzerow, "Blue phases come of age: A review," Proc. SPIE **7232**, 723205 (2009).